Digital twin in high throughput chromatographic process development for monoclonal antibodies

Silva, Tiago Castanheira; Eppink, Michel; Ottens, Marcel

DOI
10.1016/j.chroma.2024.464672

Publication date
2024

Document Version
Final published version

Published in
Journal of Chromatography A

Journal of Chromatography A 1717 (2024) 464672

Contents lists available at ScienceDirect

Journal of Chromatography A

journal homepage: www.elsevier.com/locate/chroma

Digital twin in high throughput chromatographic process development for monoclonal antibodies

Tiago Castanheira Silva [a], Michel Eppink [b,c], Marcel Ottens [a,*]

[a] Department of Biotechnology, Delft University of Technology, van der Maasweg 9, Delft, 2629 HZ, the Netherlands
[b] Downstream Processing, Byondis B.V., Microweg 22, 6503 GB, Nijmegen, the Netherlands
[c] Bioprocessing Engineering, Wageningen University, Droevendaalse steeg 1, 6708 PB, Wageningen, the Netherlands

ARTICLE INFO

Keywords:
Harvest High-throughput screening
High-throughput process development
Lumped kinetic model
Overall mass transfer coefficient

ABSTRACT

The monoclonal antibody (mAb) industry is becoming increasingly digitalized. Digital twins are becoming increasingly important to test or validate processes before manufacturing. High-Throughput Process Development (HTPD) has been progressively used as a tool for process development and innovation. The combination of High-Throughput Screening with fast computational methods allows to study processes in-silico in a fast and efficient manner. This paper presents a hybrid approach for HTPD where equal importance is given to experimental, computational and decision-making stages. Equilibrium adsorption isotherms of 13 protein A and 16 Cation-Exchange resins were determined with pure mAb. The influence of other components in the clarified cell culture supernatant (harvest) has been under-investigated. This work contributes with a methodology for the study of equilibrium adsorption of mAb in harvest to different protein A resins and compares the adsorption behavior with the pure sample experiments. Column chromatography was modelled using a Lumped Kinetic Model, with an overall mass transfer coefficient parameter (k_{ov}). The screening results showed that the harvest solution had virtually no influence on the adsorption behavior of mAb to the different protein A resins tested. k_{ov} was found to have a linear correlation with the sample feed concentration, which is in line with mass transfer theory. The hybrid approach for HTPD presented highlights the roles of the computational, experimental, and decision-making stages in process development, and how it can be implemented to develop a chromatographic process. The proposed white-box digital twin helps to accelerate chromatographic process development.

1. Introduction

The biopharmaceutical market has seen tremendous growth in the past 20 years, with more and more products getting approval from regulatory agencies [1,2]. Monoclonal antibodies (mAbs) are important biopharmaceuticals that are used to treat a plethora of diseases, such as different types of cancer and autoimmune diseases [2]. MAbs are produced by cell culture, where a host (typically CHO cells) produces them and releases them into the cell culture. Together with the mAbs, many different components are present in the cell culture which cannot be present in the final product. For patient administration, mAbs have to be produced in a highly pure form.

The first step for the purification of mAbs is of great importance as it aims to separate it from all components present in a cell culture (media components, cell metabolites, Host Cell Proteins (HCP), etc.). It is desired to have a purification step that can both concentrate and purify the product to a good extent, further reducing the volumes to be handled downstream. Affinity chromatography is usually the preferred option, and Protein A (ProA) ligands' specificity to mAbs and robustness makes it a very attractive process choice [3,4]. Even accounting for some disadvantages of ProA chromatography (expensive ligand, leaching of ProA) [5], efforts to dethrone this ligand as the first purification step of mAbs have been unsuccessful. Studies on the use of Cation-Exchange (CEX) and Multimodal (MM) ligands for the capture of mAbs from a complex mixture have demonstrated good results but still subpar compared to ProA results [6–8]. MM ligands are especially sensitive to

Abbreviations: BTC, Breakthrough Curve; CEX, Cation-Exchange; HTPD, High-Throughput Process Development; HTS, High-Throughput Screening; k_{ov}, overall mass transfer coefficient; LKM, Lumped Kinetic Model; mAb, monoclonal antibody; ProA, Protein A; SLDF, Solid-Film Linear Driving Force; TDM, Transport Dispersive Model.

* Corresponding author at: Department of Biotechnology, Delft University of Technology, Van der Maasweg 9, Delft, 2629 HZ, the Netherlands.
E-mail address: m.ottens@tudelft.nl (M. Ottens).

https://doi.org/10.1016/j.chroma.2024.464672
Received 10 September 2023; Received in revised form 14 January 2024; Accepted 21 January 2024
Available online 23 January 2024

changes in the loading conditions [8,9]. Further chromatographic steps are used to polish the mixture, aiming at removing remaining HCPs, leached ProA, genetic material of the host, and aggregates. These are usually done with a combination of Ion-Exchange (IEX) and/or Hydrophobic Interaction (HIC) chromatography steps [2,10,11].

Process development strategies for biopharmaceuticals often relied on purely experimental work. Over the past 30 years, and with the emergence of robotic workstations, other tools have become available for chromatographic process development that aim at the miniaturization and automation of experiments [12]. Many studies have showed the applicability of High-Throughput Screening (HTS) for process development using Liquid-Handling Stations [13–17], as well as other tools, such as Eppendorf tubes [18,19] and microfluidics [20,21]. However, a purely empirical approach is both sample and time consuming. For that reason, High-Throughput Process Development (HTPD) uses a combination of HTS and mechanistic modelling to accelerate development and minimize costs [22,23]. Ideally, one should aim at choosing the simplest model possible that still provides accurate results, as the computational data should be representative of the experimental data. More complex models will often require more experiments to calibrate but should also be more accurate [24]. This is not always the case, as Altern *et al.* showed recently that a Steric Mass Action model (generally used for Ion Exchange ligands) provided the best description of the system, for the case of one of the multimodal chromatography resins tested with mAbs, compared to models that included terms for the hydrophobic interaction [25].

HTPD is usually done using pure protein solutions to determine parameters and investigate protein adsorption behavior. Important parameters that are then used in the adsorption model are hard to define mechanistically and are usually derived from HTS experiments. For process development to be both fast and effective, it is important to understand if the screening with pure mAb reflects what happens in the presence of other components. It still hasn't been shown in literature (to the authors' knowledge) that the equilibrium adsorption behavior of mAbs remains the same regardless of being in pure form or in the presence of Harvested Cell Culture (harvest). Furthermore, many different models have been reported for the description of chromatography [26–29]. The most complex model (General Rate Model – GRM) provides a full description of the transport of the molecule through the column and its adsorption to the resin, whereas the "ideal" model only provides information on convection and adsorption equilibrium [26,28]. Lumped Kinetic Models (LKM) are less descriptive than GRM, usually lacking a detailed kinetic description of the system and several have been described [27,28] and used extensively for the description of chromatography of different solutes and are broadly applicable [30–33]. Mass transfer parameters can be determined experimentally or using different correlations [26]. Adsorption models also take many shapes and depend on the type of molecule-ligand interaction, with more complex ligands (such as MM) needing more complex models for the description of the chromatographic behavior [13,34,35].

"Digital Twins" is an overarching term that can be broadly used within the biopharmaceuticals industry [36]. They are defined as an *in-silico* equivalent of a process and can be used for different purposes, such as virtual experiments and control [37]. Digital twins are often used in manufacturing for data management and life-cycle analysis, but its use in R&D is still limited [38]. With increasing computational power, digital twins have become more and more accessible from a computational point of view. Often, software that offers the "keys-in--hand" digital twins are limited and expensive, allowing for little customization which limits the "twinning" capabilities. The use of grey/white-box models allows for unprecedented levels of customization and increases process understanding at a cost of understanding any programming language. Industry seems to be reaching the inflexion point in the adoption of these models, with more and more companies willing to invest in-house developed digital twins for process monitoring and development.

Taking into account all the design choices that can take place in process development of chromatography, this study presents a structured hybrid approach to HTPD for the capture and first polishing step of mAbs. It showcases the screening of dozens of different ProA and CEX resins and compares adsorption behavior of pure mAb and mAb in a harvest mixture for a number of selected ProA resins. It discusses the correlation of overall mass transfer parameter with equilibrium concentration. Finally, it shows the validation of the model and how the hybrid approach for HTPD helped to speed-up process development and how it can be used to screen more conditions without needing to perform experiments.

2. Theory

2.1. Hybrid approach for high-throughput process development

A hybrid approach was taken for the development of the chromatography step in this study. This kind of approach has been previously described [23], and can be applied to whole processes or to different processes or unit operations inside a larger process. The approach taken in this study is summarized in Fig. 1. In this approach, three different separate parts are considered: experimental, computational, and (the often not mentioned) decision making. The decision making is always based on information provided by the experimental or computational parts of the hybrid approach. Important decisions such as "knock-out" criteria for the resins after HTS or which model to choose can influence the duration of the process development stage. For this case, the process development stage could be translated into: HTS, mathematical modelling of chromatography, *in-silico* column experiments, column experiments for model validation, final process design.

The first stage of our approach involved the selection of different ProA and CEX resins for HTS. Since HTS was available, the selection criteria for this weren't too tight, and the criteria to leave out some resins was mainly based on operating constraints of the resins (pressure limitations, cleaning conditions, etc.) rather than adsorption parameters provided by the manufacturer. If enough sample is available and there is the possibility to HTS the resins, it is always advisable to screen the resins. There can be some unexpected positive/negative results, and to build a wide database on adsorption is always desirable. After HTS and data processing, the first "real" decision making stage arises, based on the adsorption data. Out of all the resins screened, the best candidates were the ones that showed a high enough q_{max} and with the most rectangular isotherm shape.

After, there is the need to select an appropriate model for the chromatographic system. There is an abundance of models to choose from, and the choice will depend on the case study and available resources (more complicated models require higher computational power) [26]. After the model is built, some column experiments are required to calibrate the model. The choice of the model is important since, generally speaking, the more complex a model is, the more experiments are needed for its calibration. This comes from a higher characterization of all phenomena involved in chromatography, which in turn means that more parameters need to be estimated [26]. From these column experiments, the necessary parameters are fit, finalizing the model building stage.

Finally, some *in silico* runs can be performed. This is the time to evaluate if the output of the model matches the steps defined by the user and if the model appears to be working. Provided that everything is in order, experimental runs with the same conditions as the ones from the *in-silico* runs are performed, and the results can be compared. If the results are comparable to the user's satisfaction, then different conditions can be tested and a decision on the best process for the case study can be made.

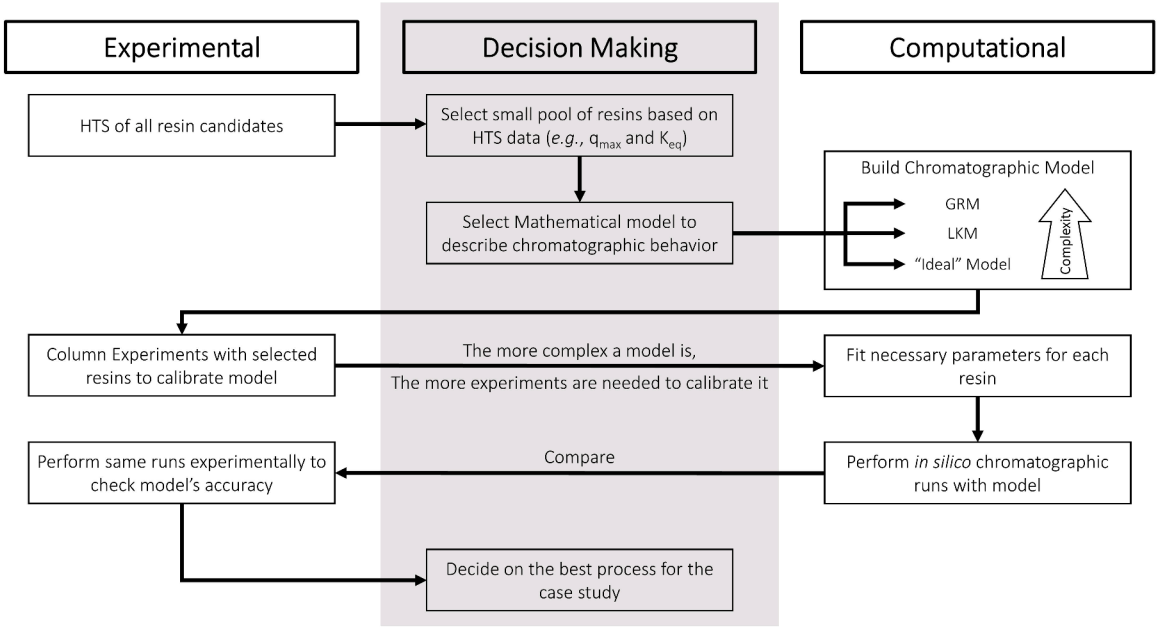

Fig. 1. Hybrid Approach for Process Development of Chromatography. HTS – High-Throughput Screening; GRM – General Rate Model; LKM – Lumped Kinetic Model.

2.2. Adsorption column model

The chosen model had to be as accurate and simple as possible. Naturally, the most complex models are very accurate, such as the General Rate Model (GRM). However, these models are often the most complex and simplifications have been proposed [39], such as the Lumped Pore Model and the Lumped Kinetic Model (LKM). For this work, the Transport-Dispersive Model (TDM) was chosen. TDM is a LKM, which in this case the simplification assumes that there are no intraparticle pores ($\varepsilon_p = 0$), meaning that there is no longer a separate mass balance for the pores. This model is simpler than the GRM but will still provide enough accuracy to describe the system, and is shown in Eq. (1):

$$\frac{\partial c}{\partial t} = -u_{int}\cdot\frac{\partial c}{\partial x} + D_L\cdot\frac{\partial^2 c_i}{\partial x^2} - \frac{1-\varepsilon}{\varepsilon}\cdot\frac{\partial \overline{q}}{\partial t} \tag{1}$$

where, c is the concentration of protein in the liquid (mg/ml), ε is the bed porosity, u_{int} the interstitial velocity of the mobile phase (m/s), and D_L is the axial dispersion coefficient (m^2/s). The mass transfer in this system is described by the Solid-Film Linear Driving Force (SLDF) model [28]. The average solid phase concentration $\overline{q}$ is described in the following equation:

$$\frac{\partial \overline{q}}{\partial t} = k_{ov}\cdot(q - \overline{q}) \tag{2}$$

Where q is the interface concentration in the stationary phase, k_{ov} is a lumped mass transfer coefficient (designated overall mass transfer coefficient) (s^{-1}).

The adsorption equilibrium can be described using many different models. The Langmuir isotherm model is a relatively simple adsorption model that is based on a number of assumptions [26], that usually can describe the adsorption of pure mixtures accurately. It is often used for affinity chromatography due to the ligands specificity. Furthermore, it is safe to assume that no competitive adsorption will happen with the ProA or the CEX ligands (for this case study), discarding the need to use more complex models. Therefore, the concentration of protein at the interface of the resin (q) is in equilibrium with the concentration of protein in the bulk of the liquid (c) and can be estimated using the Langmuir isotherm equation:

$$q_{eq} = \frac{q_{max}K_{eq}c_{eq}}{1 + K_{eq}c_{eq}} \tag{3}$$

where q_{max} is the maximum adsorption capacity (in mg/ml_{resin}), and K_{eq} is the adsorption equilibrium constant of the resin (in ml_{liquid}/mg). D_L was assumed to be 4 times the product of u_{int} and d_p, where d_p is the adsorbent's particle diameter (in m) [27,40].

The column is assumed to be free of protein at the initial time point ($c|_{t=0,\ 0\le x\le L} = 0$ and $q|_{t=0,\ 0\le x\le L} = 0$) and the boundary conditions of the column are described by the Danckwerts boundary conditions for dispersive systems [41]:

$$\text{for } x = 0 \quad c = c_{inlet} + \frac{D_L}{u_{int}}\cdot\frac{\partial c}{\partial x} \tag{4}$$

$$\text{for } x = L \quad \frac{\partial c}{\partial x} = 0 \tag{5}$$

where x the axial position, and L the length of the column. The column was modelled as a loading-elution operation, with c_{inlet} given by:

$$\text{for } t_{Eq} \le t \le t_{Eq} + t_{pulse} \quad c_{inlet}(t) = c_{feed} \tag{6}$$

$$\text{for } t_{Eq} > t$$

$$\text{or } t > t_{Eq} + t_{pulse} \ c_{inlet}(t) = 0 \tag{7}$$

where c_{inlet} is the feed concentration of protein, and t_{Eq} and t_{pulse} are the equilibration time and pulse time, respectively. The pulse duration is given by $t_{pulse} = \frac{V_{inj}}{F_{vinj}}$, where V_{inj} is the injection volume and F_{vinj} the volumetric flow rate of the injection step.

The partial differential equation (Eq. (1)) is dependent on time and axial position. Spatial discretization using the method of lines was used to transform the partial differential equations (PDEs) into ordinary differential equations (ODEs). The first and second order spatial derivatives were discretized using a fourth-order central difference scheme, with 100 grid points (N), and a step size of $\Delta x = \frac{L_c}{N}$, where L_c is the length of the column. This ODE together with SLDF equation ODE comprise the set of ODEs to be solved. The set of ordinary differential equations was solved in MATLAB® R2021a using *ode15s* as the ODE solver.

3. Materials and methods

3.1. Materials

The monoclonal antibody (M_w of 148 220 Da, pI ≈ 8.6) used in this study was provided by Byondis B.V., Nijmegen, The Netherlands, both in purified form and with the Clarified Cell Culture (harvest). The mAb used was very stable under harsh operating conditions of pH and temperature [42]. A summary of the resins used for the HTS studies can be found in Table 1.

For breakthrough curve (BTC) experiments, 1 ml MAbSelect SuRe pcc (MSSpcc) and MSPrismA HiTrap® columns from Cytiva, Uppsala, Sweden, were used. The bed height is 25 mm, the inner diameter 7 mm, and the bed volume 1 ml. The MSS column was packed using the resin mentioned above in an Omnifit™ column housing from Thermo Fisher Scientific, Waltham, MA, with an inner diameter of 6.6 mm, a bed height of approximately 2.8 cm and a bed volume of approximately 0.96 ml. The asymmetry of all columns was measured with a pulse experiment using 25 µl of a 1 % acetone solution and a 1 M NaCl solution, and was within specifications for all columns.

3.2. Buffers and solutions preparation

The different buffers and solutions were prepared by dissolving the appropriate amount of chemicals in Milli-Q water. For the protein A resin studies, a 1x Phosphate Buffer Saline (PBS) buffer was prepared and the pH corrected to 7.14 for all the experiments, to mimic the pH values of the harvest solution. For the CEX resin studies, a 25 mM NaOAc solution with 20 mM NaCl at pH 4.5 was prepared, to mimic the solution properties of the eluate of protein A after viral inactivation and subsequent pH correction. The elution buffers used for the protein A and CEX resins were 25 mM NaOAc, pH 3.5 and 25 mM NaOAc with 1 M NaCl, pH 4.5, respectively.

The provided mAb in purified form was buffer-exchanged to the buffer solutions mentioned above (depending on the resins studied) and diluted until the desired concentration was achieved. This was done using Vivaspin® 15 Turbo Centrifugal Concentrator from Sartorius (Gottingen, Germany) or Amicon® ultra-15 centrifugal filters from Merck KGaA (Darmstadt, Germany). A highly concentrated solution of mAb in PBS buffer was used to increase the concentration of mAb in the harvest for the HTS experiments using the harvest.

Table 1
Summary of the resins used in the HTS studies.

Mode	Resin name	Manufacturer
ProA	MAbSelect SuRe (MSS)	Cytiva, Uppsala, Sweden
	MAbSelect PrismA™ (MSPrismA)	
	MAbSelect SuRe LX (MSSLX)	
	Capto™ L	
	Eshmuno® A (EMA)	Merck KGaA, Darmstadt, Germany
	CaptivA® PriMAB (CPMAB)	Repligen, Waltham, Massachusetts
	Praesto® AP (PAP)	Purolite, King of Prussia, PA
	Praesto® Jetted (PJet)	
	KanCapA (KCA)	KANEKA, Tokyo, Japan
	Amsphere™ A3 (Amsphere ProA – ASPA)	JSR Life Sciences (Sunnyvale, CA)
	Toyopearl AF-rProtein A-650F (AF650F)	Tosoh Biosciences, Tokyo, Japan
	POROS™ MabCapture™ A (POROSA)	Thermo Fisher Scientific, Waltham, MA
CEX	SP Sepharose FF (SPSephFF)	Cytiva, Uppsala, Sweden
	SP Sepharose Big Beads (SPSephBB)	
	CM Seph FF (CMSephFF)	
	Capto™ S ImpAct (CapSImp)	
	CM Sephadex C-25 (CMSeph25)	
	Fractogel® EMD COO- (M) (FractoEMD)	Merck KGaA, Darmstadt, Germany
	Eshmuno® S (EshS)	
	Eshmuno® HCX (EshHCX) (*)	
	Eshmuno® CPX (EshCPX)	
	Eshmuno® CP-FT (EshCPFT)	
	Toyopearl Mx-trp-650 M (ToyoMxTrp) (*)	Tosoh Biosciences, Tokyo, Japan
	Toyopearl CM 650-S (ToyoCM)	
	Toyopearl GigaCap-650 M (ToyoGiga)	
	CHT Ceramic Hydroxyapatite Type II Media (CHT40) (*)	Bio-Rad Laboratories, Hercules, CA
	Nuvia™ S (NuS)	
	POROS™ 50 HS (POROS50HS)	Thermo Fisher Scientific, Waltham, MA

* resins that are multimodal CEX resins.

3.3. Analytical methods

Protein concentration of pure samples was determined using a CTech™ SoloVPE® system (Repligen, Waltham, Massachusetts). The concentration, aggregation, and purity of the harvest HTS samples was determined by analytical size-exclusion (SEC) chromatography in a Acquity H-class bio system (Waters Corp., Milford, MA). 2 µl of sample was injected in a Tosoh TSKgel UP-SW3000 2 µm column (Tosoh Biosciences, Tokyo, Japan), using as running buffer a mixture of 400 mM NaCl, 15 % Isopropanol, 150 mM PO_4 buffer pH 6.2, a flowrate of 0.2 ml/min and absorbance of 280 nm. Protein concentration in the studies with pure mAb was determined using appropriate calibration curves obtained using the LHS (for the HTS studies) and the ÄKTA system (for the column studies).

3.4. Breakthrough curve experiments

The breakthrough curve experiments were performed in different ÄKTA systems: Avant 150, Avant 25, and Pure 25 (Cytiva). In both systems, tubes with an inner diameter of 0.5 and 0.25 mm were used, before and after the column, respectively. These tubes had a length of 20 and 30 cm, respectively. This amounts to a total dead volume of 54 µl, which is around 5 % of the column volume was considered negligible and not accounted for the modelling of the chromatographic system [43]. However, when dead volumes represent a higher percentage of the column volume, it is advisable that they're represented in the models, to avoid discrepancies when scaling up, as they can influence the determination of process parameters such as axial dispersion coefficients and kinetic parameters [44,45]. Protein concentrations from the ÄKTA were determined using appropriate calibration curves measured in each of the systems' UV detectors at 280 nm. BTCs at different feed concentrations (fixed flow rate) and different flow rates (fixed concentration) were performed, until a plateau in the outlet concentration was achieved (meaning the resin was saturated).

3.5. Adsorption equilibrium isotherms

Adsorption isotherms provide information on the equilibrium concentration of a solute adsorbed to a solid phase (chromatographic resin) at different liquid concentrations. To understand this, known amounts of protein and resin are contacted until an equilibrium is reached. Time to reach equilibrium can vary from system to system.

3.5.1. Batch uptake adsorption equilibrium isotherms

Batch uptake experiments contact a liquid with a given initial concentration with a known amount of resin. After sufficient time is given to the system to reach equilibrium, the concentration of the liquid phase can be measured and by using a mass balance it is possible to estimate what is the amount of protein adsorbed to the solid phase, in the conditions tested (Eq. (8)):

$$q_{eq} = \frac{V_l \times \left(c_{l,initial} - c_{eq}\right)}{V_r} \quad (8)$$

where, q_{eq} is the protein adsorbed to the resin in equilibrium (in mg/ml_{resin}), V_l is the volume of liquid (in ml_{liquid}), V_r is the volume of resin (in ml_{resin}), and $c_{l,initial}$ and $c_{l,eq}$ are the protein concentrations in the liquid phase in the beginning and after equilibrium is reached, respectively (in mg/ml_{liquid}).

Batch adsorption isotherm data was generated using a Tecan EVO Freedom 200 liquid-handling station (LHS) (Tecan, Switzerland). The LHS was equipped with an orbital mixer (Te-Shake), a multi-well plate reader (InfiniTe Pro 200), a robotic manipulator (RoMa) arm, two different liquid-handling arms (LiHa and MCA96) and a centrifuge system (Rotanta).

A known amount of resin (20.8 µL) was added to a 96-well filter plate (Pall Corporation, NY, USA) using a MediaScout® ResiQuot resin loader device from Atoll (Weingarten, Germany). To wash the resin, equilibration buffer was pipetted into the filter plate, and it was shaken for 10 min at 1200 rpm, after which the solution was removed using the vacuum system. This cycle was performed 3 times in total. Protein solutions were subsequently pipetted (600 µL) inside the well plates, and the plates were agitated at 1200 rpm until equilibrium was reached (minimum 24 h). Once equilibrium was reached, the filter plate was placed on top of a 2 mL deep-well plate (Eppendorf AG, Hamburg, Germany) and these were centrifuged together using the centrifugation system. The supernatant was transferred from the deep well plates to a UV star plate and the equilibrium concentrations were measured using the plate reader. Equilibrium concentrations were estimated using appropriate calibration curves, obtained using the LHS. The results shown for the isotherms of all resins except MSSpcc were generated using this method.

3.5.2. Equilibrium isotherms from column experiments

To determine the adsorption isotherms of MSSpcc, the resulting BTCs at different feed concentrations were used. The equilibrium concentration of the liquid phase is the feed concentration of the different trials. This is done by calculating the equilibrium binding capacity (EBC), which is the binding capacity at which 100 % of the dynamic binding capacity ($DBC_{100\ \%}$) is achieved [27]. This can be estimated by calculating the area above the BTC (which corresponds to the adsorbed protein) (Eq. (9)).

$$q_{eq} = \frac{m_{adsorbed}}{V_{resin}} = \frac{q_{EBC}}{V_{resin}} = \frac{\left(c_{feed} \cdot t_{DBC_{100\%}} - \int_0^{t_{DBC_{100\%}}} c_{out}\,dt\right) \cdot F_v}{V_{resin}} \tag{9}$$

where, c_{feed} and c_{out} are the feed and outlet concentration (in mg/ml), respectively, $t_{DBC_{100\%}}$ is the time it takes to reach 100 % of DBC (in min), V_{resin} the volume of resin (in ml) and F_v the flow rate used (in ml/min).

3.5.3. Equilibrium isotherms using harvest

Equilibrium adsorption isotherms using the Harvest were obtained by contacting a mAb containing harvest solution with different ProA resins. Two different stock solutions were used: the original harvest solution, and a "spiked" harvest solution (with a $c_{mAb} = 5$ mg/ml). This solution was only 10 % of the volume of the final "spiked" harvest solution. The isotherms experiments were performed using the same methodology described in (3.5.1 - Batch Uptake Adsorption Equilibrium Isotherms), with a few changes. Due to the inability to inject high protein content solutions in the UPLC system, a slight modification to the experimental procedure had to be done, compared to the pure mAb isotherms. After the 24 h incubation period, the filter plates were centrifuged and the supernatant collected in the deep-well plates. Then, 600 µl of elution buffer was pipetted onto the filter plates and the resin was incubated for at least 1 h. The supernatant was then collected and analyzed using the UPLC system. Contrary to the pure mAb experiments, the adsorbed mass is used to calculate the c_{eq} of the harvest HTS trials:

$$q_{eq} = \frac{m_{adsorbed}}{V_{resin}} = \frac{V_{HTS_{eluate}} \times c_{HTS_{eluate}}}{V_{resin}} \tag{10}$$

$$c_{eq} = \frac{m_{init} - m_{adsorbed}}{V_{resin}} \tag{11}$$

where $m_{adsorbed}$ is the adsorbed mass to the resin (in mg), $V_{HTS_{eluate}}$ the volume of eluate used in the harvest trials (in ml), $c_{HTS_{eluate}}$ the concentration of mAb in the eluate in the harvest trials (in mg/ml) and m_{init} the initial mass of mAb present in each well for the harvest trials (in mg).

3.6. Parameter estimation

The Langmuir isotherm parameters were regressed using the pair of c_{eq} and q_{eq} for each of the resins. This was performed using the *lsqcurvefit* function in MATLAB. The fitting function was the Langmuir isotherm, as shown in Eq. (3). The error of the fitted parameters was calculated with an appropriate error propagation, described in 3.7 - Statistical Analysis. The overall mass transfer coefficient was estimated using the experimental data from the BTC experiments at different feed concentrations. The *fmincon* function in MATLAB was used and the default tolerances (1e-6) were used for the fit.

3.7. Statistical analysis

The reported uncertainties were calculated taking into account the systematic error and the statistical error resulting from random variation of measured values. The sample standard deviation and error propagation was calculated according to Young [46]. For the systematic error, only the uncertainty associated with the parameter regression of the calibration was considered, as other equipment errors were considerably smaller and thus negligible. The error of the regressed isotherm parameters was obtained using the variance-covariance matrix M, which is calculated by multiplying the variance of the residuals of the best fit with the Jacobian matrix (J) of the fitting function, as shown in eq. (12):

$$M = \frac{\left(J^T J\right)^{-1} \sum_{i=1}^{n} res_i^2}{n - p} \tag{12}$$

where, n is the number of data points, and p the number of regressed parameters. The diagonal of the covariance matrix contains the variance of each parameter [47].

4. Results and discussion

4.1. Adsorption isotherms pure mAb

The approach mentioned in Section 2.1 was followed. The first step was the screening of the different stationary phases of both ProA and CEX ligands. This was done using pure mAb solutions, which will provide some insight into the adsorption capacity and affinity of the different resins. The buffer choices were done already considering what would be found in a manufacturing scenario: the buffer chosen for the ProA experiments mimics the pH and conductivity of the harvest solution, and the buffer chosen for the CEX experiments mimics the salt content, pH and conductivity of the solution after viral inactivation and subsequent pH correction.

4.1.1. Protein A resins

The HTS results for the equilibrium adsorption isotherms ProA ligand resins are shown in Fig. 2 (Capto® L data shown in Figure SI 1). The isotherm data were fitted using the Langmuir isotherm (eq. (3)), and the fitted values can be found in Table 2. The results show that most of the resins possess highly favorable adsorption isotherms, which is in agreement with affinity chromatography (Praesto AP and CaptivA PriMAB are the exceptions, which are still favorable but with a less rectangular profile). This is also confirmed by the high K_{eq} values for the resins, with some even in the order of magnitude of thousands. This is a mathematical artifact from the fitting of the experimental data to the

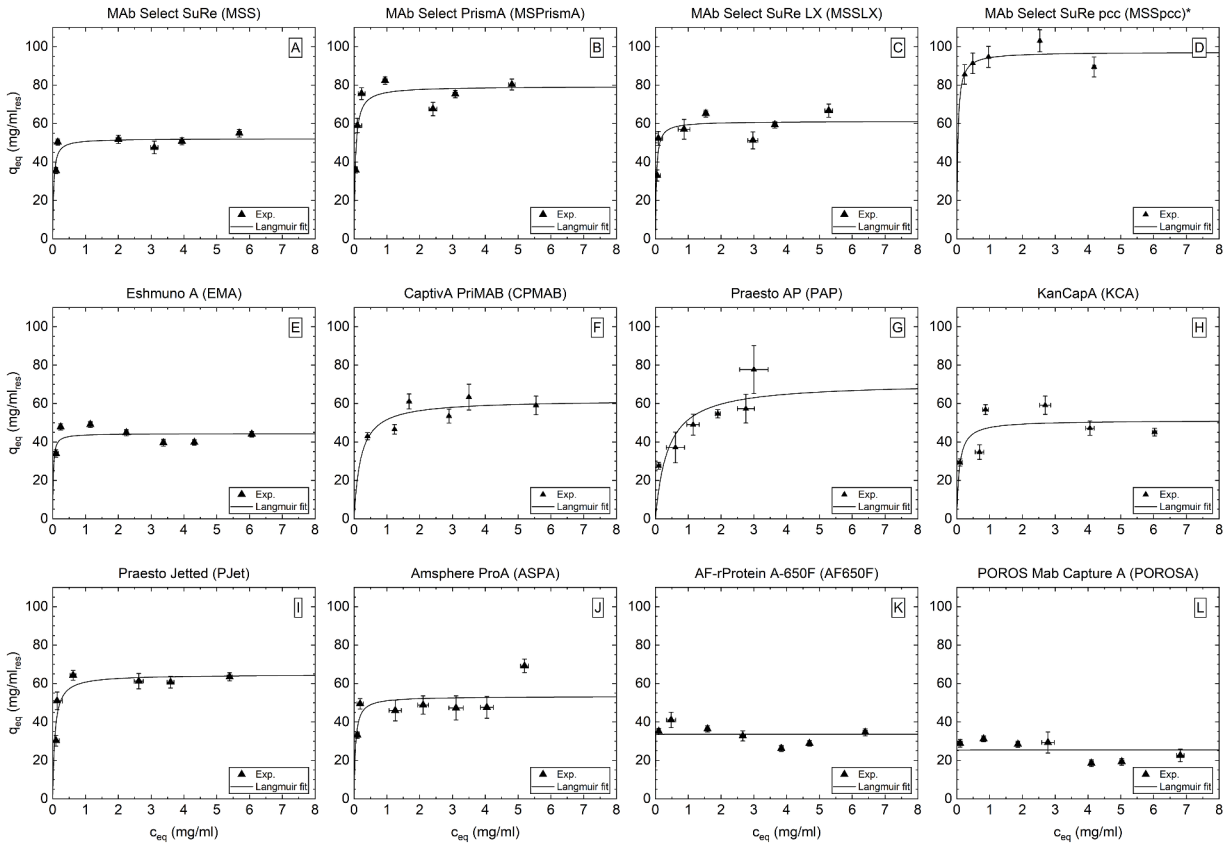

Fig. 2. Adsorption isotherms of mAb on different Protein A resins, in 1x PBS buffer, pH 7.14. Solid lines represent the fit of the experimental data to the Langmuir isotherm. A – MSS; B – MSPrismA; C – MSSLX; D – MSSpcc; E – EMA; F – CPMAB; G – PAP; H – KCA; I – PJet; J – ASPA; K – AF650F; L – POROSA.

Langmuir equation and is a consequence of the rectangular shape of the isotherm for these resins, which lack experimental points in the linear part of the isotherm, skewing the fitting.

Considering the performance of the resins, it is possible to see that MAb Select PrismA, MAb Select SuRe pcc, Praesto Jetted, and Praesto AP present the highest maximum capacity values for the studied mAb (between 65 and 95 mg/ml$_{resin}$), with MSPrismA and MSSpcc clearly outperforming the other resins and Praesto AP presenting a smaller affinity constant. CaptivA PriMAB, MAb Select SuRe, MAb Select SuRe LX, KanCapA, and Amsphere ProA all showed maximum capacity values in the middle range (between 52 and 62 mg/ml$_{resin}$), with the first presenting a smaller affinity constant than the rest. The remainder of the resins (Eshmuno A, AF-rProtein A-650F, POROS Mab Capture A, Capto® L) showed maximum capacity values in the lower range of all the tested resins (between 25 and 44 mg/ml$_{resin}$). This first screening stage served as a first step to understand which resins would be used for the isotherm studies using harvest solution.

Since the HTS for the harvest required more experimental effort, it was decided that 4 resins would be selected for the harvest study, out of the 13 resin pool: MSS, MSPrismA, MSSLX, and PJet. MSSpcc was not chosen because it was not available in bulk form (only in pre-packed column). The resins were chosen based on their maximum adsorption capacity and affinity constant. Although Praesto AP had a higher maximum binding capacity than MSSLX, the smaller affinity constant lead to it being discarded for this trial. MSS was selected because of its relevance and widespread use in industry-relevant processes.

4.1.2. CEX resins

The results with the different CEX ligands are presented in Fig. 3 (CM Sephadex C-25 and Toyopearl CM 650-S data shown in Figure SI 2). The isotherm data were fit using the Langmuir isotherm (Eq. (3)), and the fitted values can be found in Table 2. Under the operating conditions (pH 4.5), the mAb is positively charged since the pH is below the pI. This means that it is expected that the adsorption isotherms will be favorable, and that is what can be seen from the experimental data. Only for the case of CM Sephadex C-25 (**Figure SI 2**) there was virtually no adsorption of mAb to the resin. This happened because CMSeph25 is a weak CEX resin, and the recommended operating pH is between 6 and 10, which means that the ligand will not be charged at pH 4.5, thus not adsorbing any protein. Four main clusters were chosen for the CEX resins, according to their ligand/backbone characteristics: Fig. 3A shows multimodal CEX resins, Fig. 3B shows sepharose resins, Fig. 3C shows resins with SO_3^- functional group, and Fig. 3D shows resins with sulfoisobutyl and sulfopropyl functional groups.

The Langmuir fits show rectangular shapes for all the tested resins, with 3 resins showing very sharp rectangular shapes: Toyopearl MX-trp-650 M and Fractogel EMD COO^- in Fig. 3A and D, respectively, and Toyopearl CM 650-S in **Figure SI 2** right. For the last two resins, this is mainly a mathematical artifact from the Langmuir fit due to a lack of experimental data points in the low c_{eq} range. However, for Toyopearl MX-trp-650 M there is a large amount of data over the low c_{eq} range with corresponding high values of q_{eq}, which then decrease at high c_{eq} values. Since the Langmuir fit is made for isotherms that have an asymptote shape (with cap on the fitted q_{max} value), the fit will then converge to the values of q_{max} and K_{eq} that minimize the error, resulting in such a Langmuir isotherm shape. From the manufacturer's data it is clear that the pH can influence drastically the adsorption capacity of ToyoMxTrp, with a pH change from 4.8 to 5 decreasing the binding capacity as much as 60 % (from approx. 95 to 35 mg/ml) in a solution at roughly the same ionic strength [48]. Antibodies possess tenths and even up to one hundred buffering amino acid side chains per molecule [49], which means that despite the buffer's pH being 4.5, the solution's pH at higher mAb concentrations may be different than the target 4.5. For experiments at higher c_{eq} a higher initial concentration of mAb is present in each well,

Table 2
Summary of the Langmuir parameters fitted to the experimental data of mAb adsorption isotherms to the different Protein A and CEX resins.

ProA Resin	q_{max} (mg/ml$_{res}$)	K_{eq} (ml/mg)
MSS	52.17 ± 1.15	34.39 ± 7.82
MSPrismA	79.35 ± 1.66	23.82 ± 3.27
MSSLX	61.19 ± 1.31	33.18 ± 5.62
MSSpcc	97.25 ± 2.02	31.79 ± 11.65
EMA	44.39 ± 0.96	55.23 ± 20.82
CPMAB	61.92 ± 1.82	5.00 ± 1.13
PAP	70.92 ± 5.32	2.66 ± 0.91
KCA	51.23 ± 2.32	12.75 ± 4.61
PJet	64.69 ± 1.75	15.30 ± 2.60
ASPA	53.32 ± 1.83	22.40 ± 6.98
AF650F	33.57 ± 0.96	9.87E+03 ± 7.21E+05
POROSA	25.47 ± 1.00	7.95E+03 ± 6.52E+05
CaptoL*	38.20 ± 2.12	66.20 ± 68.93
CEX Resin	**q_{max} (mg/ml$_{res}$)**	**K_{eq} (ml/mg)**
CHT40	11.13 ± 0.62	14.39 ± 20.72
EshHCX	106.89 ± 2.31	24.47 ± 4.12
ToyoMxTrp	82.04 ± 6.37	5.96E+03 ± 7.23E+04
SPSephFF	98.68 ± 0.66	49.74 ± 2.55
SPSephBB	75.48 ± 2.04	53.83 ± 15.80
CMSephFF	69.10 ± 0.72	126.44 ± 12.81
NuS	150.64 ± 9.80	106.75 ± 29.86
CapSImp	81.70 ± 0.52	86.66 ± 4.69
EshS	125.09 ± 6.26	74.45 ± 20.30
ToyoGiga	131.05 ± 4.09	73.86 ± 11.90
EshCPX	76.01 ± 0.84	109.07 ± 10.61
EshCPFT	66.17 ± 0.55	126.67 ± 10.92
FractoEMD	21.82 ± 1.56	9.70E+03 ± 1.36E+07
POROS50HS	52.47 ± 0.76	234.49 ± 44.18
CMSeph25**	0.00 ± 2.76E+07	0.00 ± 5.21E+04
ToyoCM**	19.84 ± 1.18	9.68E+03 ± 4.22E+06

* Isotherm of CaptoL shown in SI.
** Isotherms of CM Sephadex 25 and Toyopearl CM 650-S shown in SI (these resins have a functional group of carboxymethyl).

possibly leading to a stronger effect of the buffering capacity of the mAb in the solution's pH value, explaining the lower q_{eq} values for this resin at higher mAb concentrations.

The resins with the SO_3^- functional group showed the highest maximum capacity of the different clusters, whereas the resins with sulfoisobutyl and sulfopropyl functional groups showed the most variability between the resins in terms of maximum capacity. It was expected that the adsorption capacity of SP Seph FF and SP Seph BB would be similar since the resins have the same ligand. However, we see that the adsorption of SP Seph BB is inferior to what is observed to SP Seph FF. Although the resin beads of SP Seph BB have a particle diameter of 100–300 μm, which is bigger than the 45–165 μm of SP Seph FF, the resins have different pore sizes, with pore size of SP Seph BB being reported at around 7 nm [50] and SP Seph FF pore size being reported at around 60 nm [51]. It is hypothesized that the smaller pore size hinders protein transport inside the SP Seph BB resin beads, thus preventing more protein to adsorb to the binding sites closer to the core of the resin leading to lower adsorption being observed.

Overall, the screening of CEX resins with pure solutions of mAb suits a logical choice for process development since it is expected that the solution will already be very pure after the ProA step. The same rationale applies to the buffer choices, since the goal is to have less buffer-exchanges in the whole purification train, as these are time consuming and expensive steps. There could be a more suitable buffer for each of the resins, but by choosing this buffer it is guaranteed that operationally it will require very little manipulation after the viral inactivation step. Furthermore, it was decided that no additional screening with CEX resins was needed since the goal was to generate a database that could handle a CEX step after a ProA step, and the ProA step generates a highly pure sample of mAb (confirmed by the results of the harvest adsorption equilibrium experiments). In addition to the mentioned study, analyzing the stability of the proteins when adsorbed to the resin is another criteria for narrowing down the resin selection.

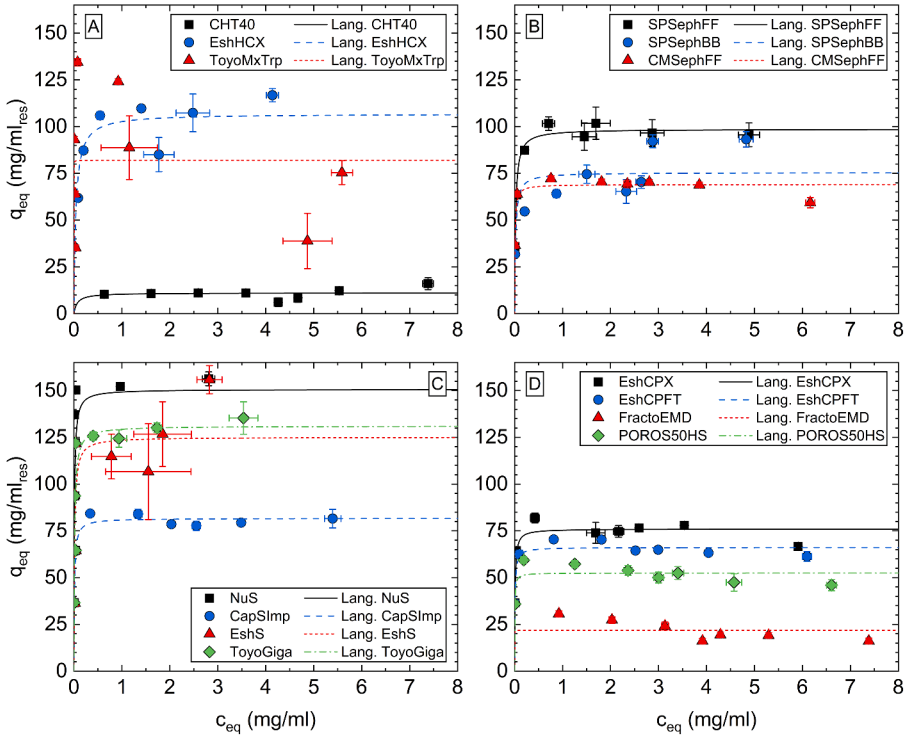

Fig. 3. Adsorption isotherms of mAb on different CEX resins in 25 mM NaOAc buffer, pH 4.5. A – Multimodal CEX resins; B – Sepharose resins; C – -SO3$^-$ functional group resins; D – Sulfoisobutyl (Eshmuno CPX and CPFT and Fractogel EMD COO$^-$) and sulfopropyl (POROS 50 HS) functional group resins).

4.2. Adsorption isotherms harvest – protein A resins

Although the pure mAb experiments already give a good indication on the maximum binding capacity and affinity constants of each resin, it is important to understand if the adsorption behavior of mAb in harvest or pure solutions changes. To achieve this, it was decided to perform HTS with mAb in a harvest solution, using similar methodology to the one described for the pure mAb approach. Since the flowthrough of the filter plates for these experiments is a harvest solution with a multitude of components, a calibration curve using the UV plate reader was not possible.

Therefore, for the analysis of the equilibrium concentrations, the UPLC was used. However, the method used was SEC-UPLC and not Analytical Protein A Chromatography (APAC). In turn, this means that the equilibrium solutions could not be injected directly in the column due to their high protein content. Consequently, after incubation was achieved, the equilibrium solution was collected in a deep-well plate and the resin present in the 96WP was incubated with elution buffer, to desorb all mAb that adsorbed during the first incubation. After sufficient time was given for the desorption of mAb, the solution was collected in a different deep-well plate and the concentrations were measured using the SEC-UPLC. This means that, contrary to what happened for the pure mAb, this measurement provides information on what was adsorbed to the resins, rather than what remained in solution. The 4 resins chosen for the harvest study were MSS, MSPrismA, MSSLX, and PJet. The reasoning behind the selection of these resins is discussed in Section 4.1.1.

The results of the adsorption equilibrium isotherms with the harvest solution are shown in Fig. 4. The results show very good agreement between the pure mAb experiments and the harvest solution experiments. Even though the harvest solution experiments required extra experimental steps, this seems to not have affected the results. These results also confirm what had been seen for the pure mAb experiments, with MSPrismA showing higher maximum adsorption capacity than the other three resins.

The results from Fig. 4 show that, for most resins, the harvest experiments isotherms would have a slightly less sharp profile. On the one hand, the methodology used for the determination of the concentration of samples of the harvest experiments is more accurate than the one used for pure mAb samples (UPLC and spectrophotometer, respectively). On the other hand, the experiments for the harvest trials required more steps, such as an elution, leading to more possibilities of the introduction of experimental error. This is observable when looking at the lower and higher equilibrium concentration parts of the isotherm for the harvest (as evident, e.g. in Fig. 4B), where there is a visible discontinuity between lower and higher liquid equilibrium concentration.

A lower experimental volume of eluate than the theoretical would affect all data points in the isotherm alike. This systematic error affects the determination of the equilibrium concentrations in the same ratio (in the solid and liquid phase), which in absolute terms will be more pronounced the higher the absolute value of the concentration. This results in a higher shift to the left of the data points in the higher q_{eq} values of the linear part of the isotherm, leading to a higher slope of the isotherm. Isotherms with high slopes have also been reported elsewhere [19]. Furthermore, it has been observed that the chromatographic behavior between pure samples and harvest samples is very similar, thus the initial slope of the isotherm should be the same for both harvest and pure samples, and the experimental differences aforementioned can help explain the difference in the isotherm profiles. The harvest data shows that the screening with the pure mAb gives enough confidence in the estimation of relevant adsorption parameters for ProA resins. This implies that for future ProA-based process development it is most likely not necessary to screen resins using the harvest solution.

4.3. Column experiments

Following the hybrid approach described in Section 2.1, after the first screenings and model choice are done, it is time to perform some column experiments (BTC) with the selected resins to calibrate the model. These usually involve, but are not limited to, experiments with

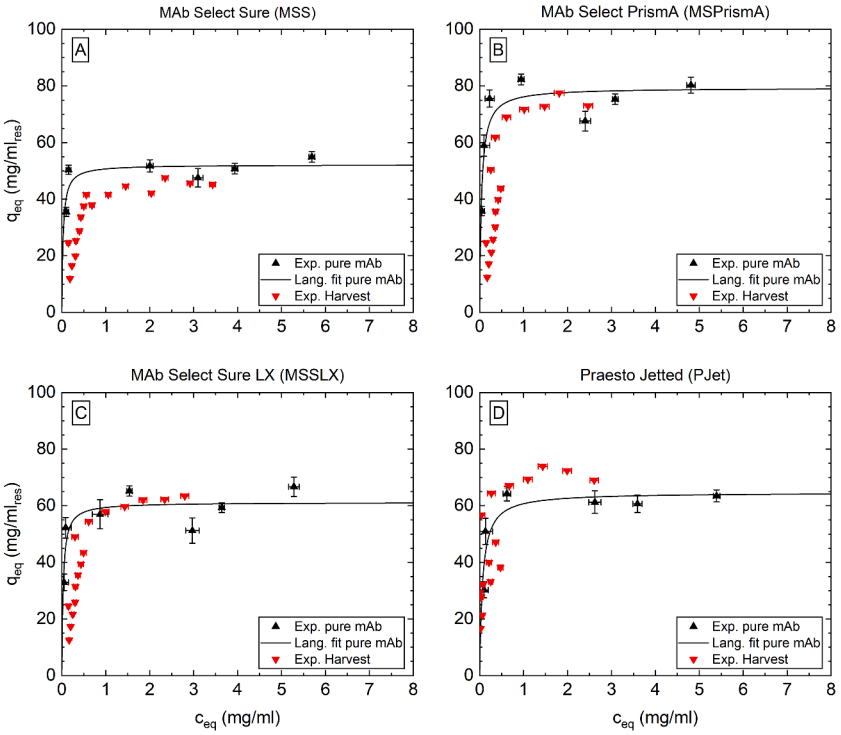

Fig. 4. Comparison of the adsorption of mAb to four different Protein A resins from pure sample and harvest. A – Mab Select SuRe (MSS); B – Mab Select PrismA (MSPrismA); C – Mab Select SuRe LX (MSSLX); D – Praesto Jetted.

varying loading concentration and constant flowrate and with constant loading concentration and varying flowrate. These experiments first serve as a check of the model suitability and, if that is confirmed, to estimate or fit some parameters that cannot be determined using mathematical correlations. In the case of the present work, these experiments were used to estimate the overall mass transfer coefficient of our system, since the axial dispersion coefficient was estimated using the correlation mentioned in Section 2.2.

The BTCs for MSPrismA are shown in Fig. 5 and for MSS and MSSpcc are shown in **Figure SI 3**. MSPrismA and MSSpcc were chosen because they showed the highest maximum adsorption capacity and MSS as the industry standard. The results of the experimental BTCs are in line with the expected results. As it can be seen in Fig. 5A, for less concentrated solutions, more column volumes (CV) will have to be flowed through the column to saturate all the resin's binding sites. Fig. 5 shows the BTCs at different flowrates (and, therefore, different residence times). It is noticeable that at higher flowrates (lower residence times), there is earlier breakthrough of protein from the column, and the shape of the BTC is less sharp (flatter). This can be attributed to the shorter times allowed for adsorption to take place, since the residence time is shorter. Other authors have also reported that some resins present a decrease in DBC with decrease of residence times [52–54]. A flatter BTC will lead to an under-utilization of the resin in the column since less CV will be required to reach the defined%DBC defined for the process. The flowrate (or residence time) is an important parameter for the design of chromatography, mainly due to its influence in the shape of BTCs. This becomes increasingly important in the design of continuous chromatography systems that do not operate in flowthrough mode.

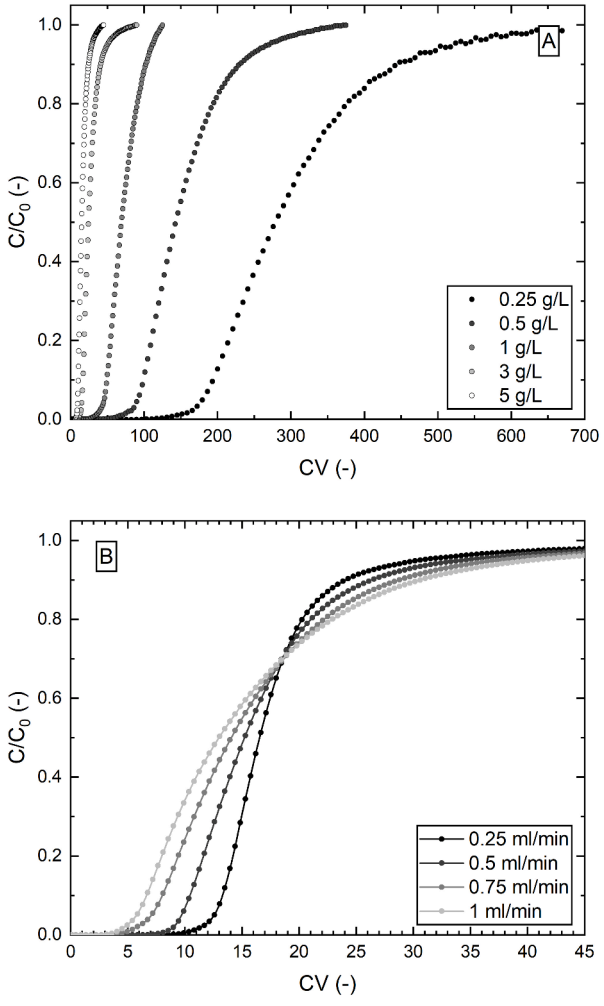

Fig. 5. Column experiments used for the calibration of the mechanistic model for MSPrismA with pure mAb solutions. A - Different initial concentration and constant flow rate (F_v = 0.5 ml/min); B - Different flow rate and constant concentration (c_{mAb} = 5 g/L). Dots represent 100 data points from every experiment. In B, the line connecting the experimental data points is used to guide the reader's eye. C/C_0 – normalized concentration (concentration observed divided by inlet concentration). CV – column volumes.

4.4. Parameter estimation

The selected model for mass transfer in the present work was a lumped-parameter model. These models assume that changes in the concentration occur very near to the boundary of the solid-liquid interface but that far from this interface the system is "well-mixed", so that the concentration in the solid and liquid interface does not change the further we are from the interface [55]. It was assumed that the kinetics of adsorption and desorption was much faster than the mass transfer kinetics, therefore the model used was the Transport-Dispersive Model [28]. In the SLDF model, all contributing mechanisms for band broadening are lumped in a coefficient, which in the case of this work is defined by k_{ov}. The lumped phenomena include pore, solid, and free diffusivities, film mass transfer coefficient, among others [26,28].

Correlations have been proposed to describe the overall mass transfer coefficient of LKMs, for example, based on the external film mass transfer coefficient [56], and have been extensively used [29,31]. These correlations are proposed for the liquid-film linear driving force model. For the current work this was not applicable, since the SLDF was used.

Ruthven has described that the diffusivities are not independent of the solute's concentration, at either low or high solute concentration [56]. A recent study by Yu et al. also found that the diffusion coefficient of proteins is a function of the protein's concentration in solution, with a higher diffusion coefficient in more concentrated solutions [57]. For the SLDF model, concentration dependence between the rate coefficient and solute concentration has been previously described [28,58,59]. Furthermore, recent work has described this dependence in the rate coefficient expressions, for example with the rate depending on the partition ratio, which in turn depends on the solute concentration [60]. Other authors have also described this correlation in terms of mathematical equations for constant pattern behavior [61]. Furthermore, it has been reported that apparent diffusion coefficients are dependent on the isotherm chord, which in turn is dependent on the solute's concentration [28].

Therefore, it was concluded that the rate coefficient, in this case the overall mass transfer coefficient, had a concentration dependence. To evaluate this, the k_{ov} was fit to BTCs with varying protein concentration. The obtained values for k_{ov} VS c are shown in Fig. 6. Comparing the results of the three different resins tested, it is noticeable that the obtained values are different from resin to resin. This was expected because there are different phenomena playing a role in the mass transfer in chromatographic separations, from pore diameter, particle radius, among others, and these depend on the resin's characteristics. The results obtained from this work's estimation are similar to the ones obtained by Chen et al. [61], even though the authors present a modification to the model described by LeVan and Carta [60].

The fitting of k_{ov} to the experimental BTC was easily achieved and provided results with good confidence intervals. This method of determining the mass transfer coefficient eliminates the need to have laborious mathematical descriptions for this parameter, whilst providing accurate results without requiring extra experiments. The linearity of the correlation could be easily implemented in the model and provided good forecasting abilities even for concentrations that were not tested experimentally, thus adding to the predictive capabilities of the model.

The k_{ov} estimated in the context of this work is a function of the feed concentration and it represents the k_{ov} averaged over the length of the column over the time it takes to fully saturate the column in the context

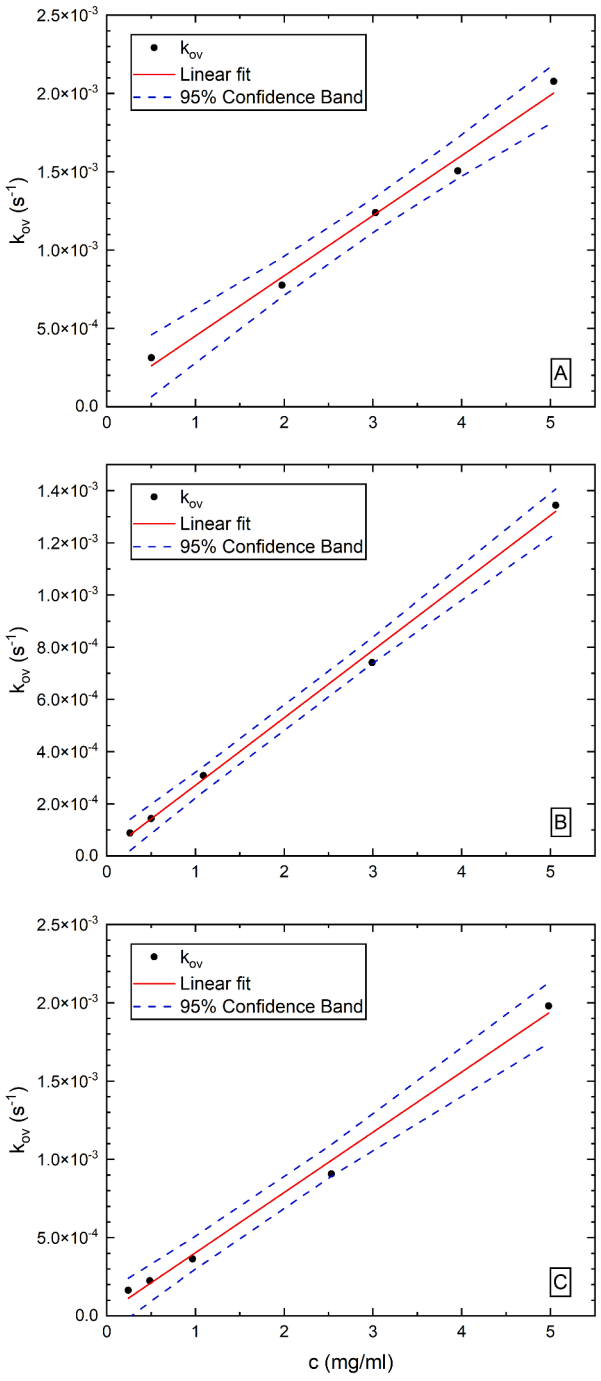

Fig. 6. Variation of k_{ov} with concentration for 3 different Protein A resins. A – MSS; B – MSPrismA; C – MSSpcc. The red line (—) represents the linear fitting and the blue dashed lines (- - -) represents the 95 % confidence band of each fitting.

of BTC experiments. This is, of course, a simplification of the physical phenomena responsible for mass transfer and adsorption inside the column. In reality, with the aforementioned references, the mass transfer parameters are a function of protein concentration. Since protein concentration changes along the length of the column and with time, due to the progression of the protein front through the column and the protein that gets retained through adsorption, one could say that the overall mass transfer coefficient (or any mass transfer coefficient, for that matter, such as film mass transfer coefficient or pore mass transfer coefficient) depends simultaneously on feed concentrations, axial position, and time. The inclusion of this dependence in the k_{ov} parameter would increase the complexity of the fitting while not improving the accuracy of the model. The model presented in this work aims at providing the most accurate results possible with the simplest possible model, while still maintaining physical description of the system. The proposed correlation between k_{ov} and feed concentration achieved this goal, hence why it was decided to use the presented model for the current study.

4.5. Model validation

In Fig. 1 it is highlighted that the first "Computational" task is the choice of the model. In this step, prior knowledge of the system and of chromatography in general can play an important role into making a first choice of model as close to an appropriate one as possible. The LKMs offer detailed descriptions of chromatographic behavior at a low computational expense, compared for example with the GRM. The LKMs can be described by Linear Driving Force (LDF) models, based either on the liquid or solid phase concentration of protein. In the case of linear isotherms, the results are not expected to change much between the two LKM [27,56]. However, the same does not hold for non-linear isotherms, which is almost always the case for the biopharmaceutical industry. For systems with favorable adsorption isotherms it has been described that the SLDF model is preferred when intra-particle resistance is the dominant mass transfer resistance [27]. In the case of this work, the film (external) mass transfer resistance was considered negligible compared to the internal mass transfer resistance [62]. The fit (or misfit) of the experimental results with the model's results can prove/disprove the validity of the assumptions taken and, in case the assumptions were not correct, a re-evaluation of the chosen model may be needed.

Following the steps described in Fig. 1, after fitting the necessary parameters to the model, the first *in-silico* runs can be performed. These runs serve as a first screening step to understand if there are any major flaws in the model. This is done based on the output chromatogram and how this looks. After the experimental conditions are set *in-silico*, the same experiment can be run in the chromatographic equipment in order to understand if the model's and experiment's results are in agreement. Fig. 7A shows the validation of the model, by comparing a loading step to 100 % breakthrough of a 5 g/L mAb solution. It is possible to see from the experimental results that the model was able to capture the adsorption behavior accurately, with a good prediction of the initial breakthrough and the shape of the BTC. Similar results were achieved for the other two resins (data not shown).

The model was able to capture the essence of the chromatogram for all the different steps. The loading behavior (the most important step) was accurately described as discussed above. The washing profile was also consistent to what is expected, with a decrease in the concentration of protein at the outlet of the column, consistent to what is expected experimentally, since the non-adsorbed mAb present in the interstitial fluid flows out of the column during the wash step. The model also shows a sharp elution profile with a little tailing. This is consistent with ProA elution profiles, which generally use low pH solutions as modifiers that will make the mAb almost instantly elute, generating a very concentrated protein front, which then tails off due to axial dispersion. Simulations with different loading volumes showed results consistent to what is expected. When loading the column to $DBC_{10\ \%}$ and $DBC_{50\ \%}$ (Fig. 7B and C, respectively) the elution peaks were smaller than for $DBC_{100\ \%}$, with $DBC_{10\ \%}$ and $DBC_{50\ \%}$ having the smallest and second smallest elution peaks, respectively, which was expected due to the lower amount of mAb loaded onto the columns.

4.6. Model application: preparing for higher USP titers

The applicability of chromatography models in the biopharmaceutical industry has been thoroughly discussed [63]. Increasingly higher titers in the Upstream Processing have shifted the costs to Downstream Processing, of which ProA represents a big portion of the costs [2,5]. The

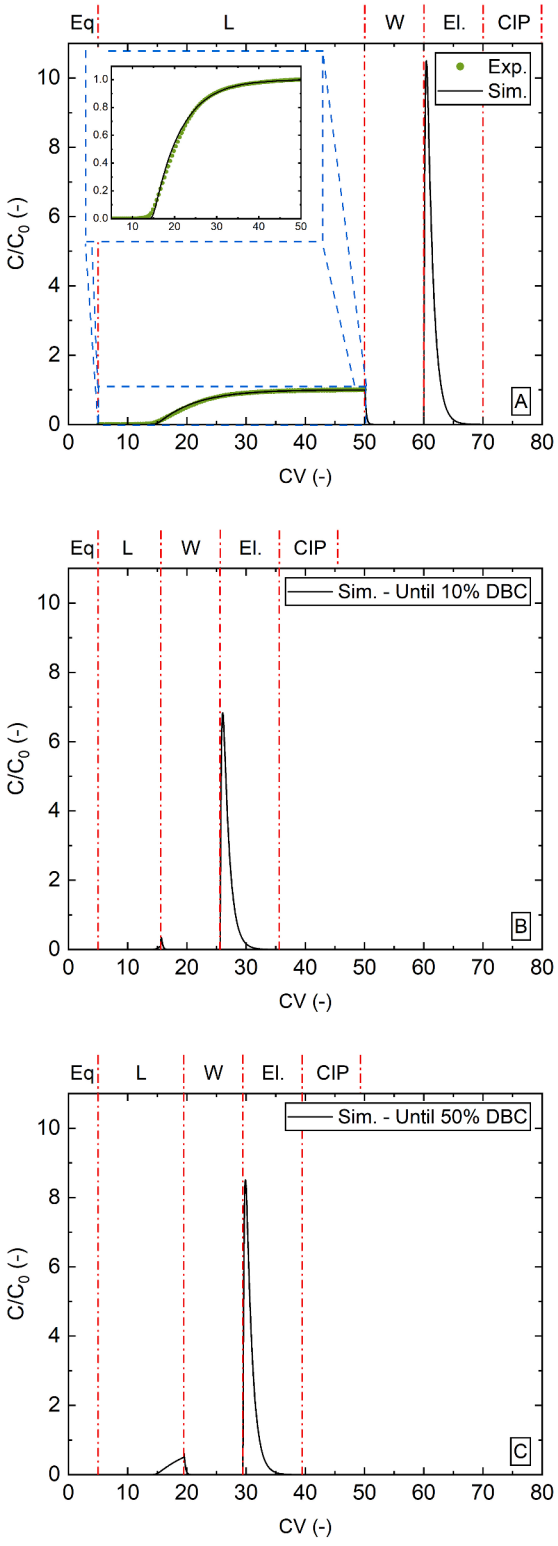

Fig. 7. Validation of the used mechanistic model for the simulation of protein chromatographic behaviour with MSPrismA at a loading concentration of 5 g/L and a loading flow rate of 0.5 ml/min. A – Model validation by loading the column to 100 % Breakthrough: experimental data points (•); B & C – Example of model applicability, by testing the loading of the column until 10 % and 50 % Breakthrough, respectively. Vertical red dash-dot lines (–•–) represent the different phases. Different column volumes were used for different phases: Equilibration (Eq.) – 5 CV, Load (L) – variable, Wash (W) – 10 CV, Elution (El.) – 10 CV, CIP – 10 CV. These are represented above each plot.

approach followed in this work showed how chromatographic process development could be tackled, from beginning to end.

The model showed good results for a variety of feed concentrations (data not shown), of which a comparison between model and experimental results are shown for a 5 g/L feed concentration. This concentration was chosen because it is becoming an industry standard to achieve such titers of mAb during cell culture. Since ProA is the first step in the purification of mAbs, it is important to have a good mechanistic understanding of the process, which the results above show. Furthermore, and considering how much titer has increased throughout the last two decades [2], a model that can accurately predict this increase in feed concentration is important for process design and is provided in this work.

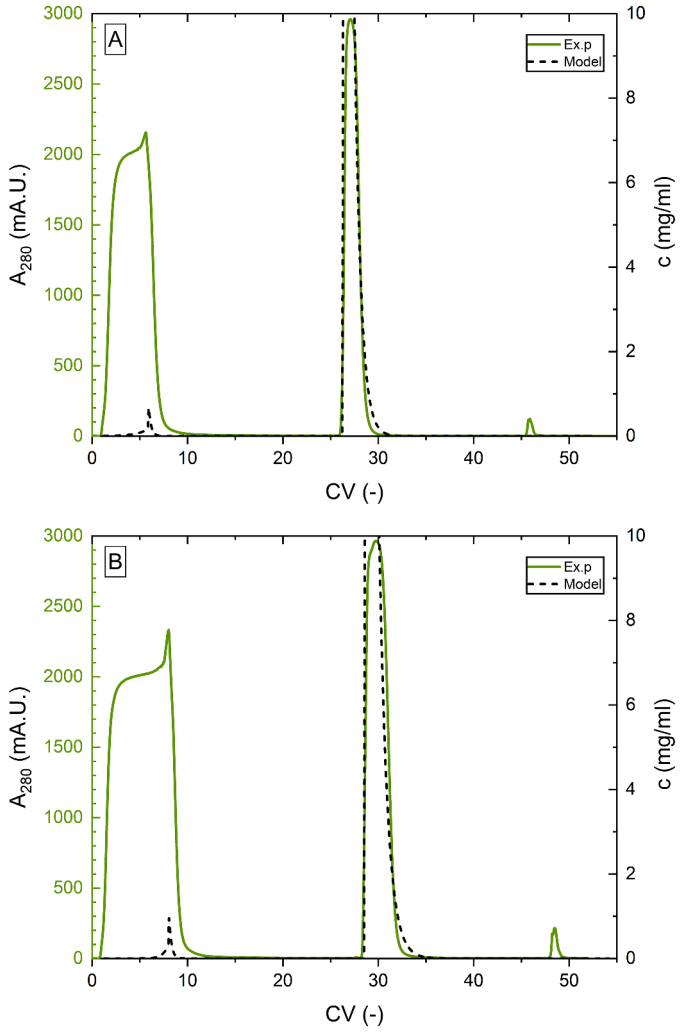

Fig. 8. Purification of the mAb from harvest solution using MSS (A) and MSPrismA (B) with a titer of 5 mg/ml and a flowrate of 0.49 and 0.68 ml/min, respectively. Experimental data is given in Absorbance Units (mA.U.) and model data is given in concentration (secondary y-axis). Model data was obtained for a pure mAb scenario, since the impurities were not modelled. Initial breakthrough of mAb can be observed by the slight shift in the plateauing curve during loading (approximately at around 2000 mA.U.) and was accurately predicted by the model. Elution was also accurately predicted by the model. There are some discrepancies between experiments and model in the CIP, since in the model it is assumed that no mAb is lost in this phase. The used volumes for each phase were: Loading – 4.7 CV (MSS – A) and 8 CV (MSPrismA – B); Wash – 20 CV; Elution – 15 CV; CIP – 10 CV. UV signal saturated at 3000 mA.U., which would correspond to a 10 mg/ml solution in case the used calibration would be extrapolated to the maximum mA.U. value, hence why the maximum of each axis was set to these values.

To provide further clarity on this, a mAb at a titer of 5 mg/ml was purified from a harvest solution using a ProA resin (Fig. 8). The experimental results show a great initial increase in the UV signal due to the presence of impurities in the harvest solution. This signal starts plateauing at around 2000 mA.U. and after some CV, there is again an increase in the UV signal, marking the beginning of breakthrough of mAb, which is clearly captured by the model. Model results were generated for pure mAb solutions since it was considered that for a purification scheme that includes a ProA step it would be unnecessary to attempt to model the interactions between the ProA resins and the components in the harvest solution. Elution results also show good agreement between model data and experimental data. CIP shows that some mAb was stripped from the column in the experiment and not in the model. This is because when modelling this step, it was considered that all mAb would be removed in the elution phase. Nonetheless, the amount of mAb in the CIP is negligible compared to the elution phase.

The proposed model showed that with a small number of experiments it is possible to reach an accurate model. With the linear mass transfer coefficient correlations, it would even be possible to extrapolate the results to calculate a k_{ov} for higher concentrations, with an experimental check being recommended. The obtained results are pivotal for the design of the capture step. Anything ranging from appropriate loading flowrate, to Yield and productivity predictions and capacity needed, can be predicted using the developed model. In addition to what was described, models are great tools that can be used for the control of chromatographic processes, provided that they are accurate and fast enough [64]. The capabilities of this model in accurately predicting chromatographic behavior highlight its use as a Digital Twin for the chromatography step. The step can be further studied and optimized *in-silico* by varying a multitude of parameters, from flowrates to feed concentrations or column dimensions, without the need to test every design idea experimentally. This reduces the experimental burden in early development stages, helping to achieve the desired process faster and cheaper. Furthermore, such chromatographic models help to enhance process knowledge and helps to achieve a Quality by Design approach in biopharmaceutical process development.

5. Conclusions

This work focused on the development of a hybrid approach for the development of a chromatographic step for the purification of monoclonal antibodies (Fig. 1). This approach focused on minimizing experiments and applying mechanistic models that are as simple as possible whilst providing a good prediction for the chromatographic behavior. The approach made use of HTS of several resins (both ProA and CEX) and the development of a mechanistic model for chromatography.

The choice of model used to study mAb chromatography was based on achieving the best description of the chromatographic behavior with the least complexity possible. A LKM with SLDF model, using Langmuir adsorption model, was used and the overall mass transfer coefficient was determined through breakthrough curve (BTC) experiments. The linear correlation between feed concentration and the mass transfer coefficient simplified the model compared to other methodologies proposed for the estimation of this parameter [60,61]. This linear correlation can be used to extrapolate the overall mass transfer coefficient for solutions with a higher mAb concentration, provided that there is experimental validation. The model results were then compared to an experiment and showed great agreement between the model's predictions and the experimental results at a feed concentration of 5 g/L, showing the model's validity and applicability.

CRediT authorship contribution statement

Tiago Castanheira Silva: Writing – original draft, Methodology, Investigation, Data curation, Conceptualization. **Michel Eppink:** Writing – review & editing, Supervision, Resources, Investigation, Conceptualization. **Marcel Ottens:** Writing – review & editing, Supervision, Resources, Project administration, Investigation, Funding acquisition, Conceptualization.

Declaration of competing interest

The authors declare that they have no known competing financial interests or personal relationships that could have appeared to influence the work reported in this paper.

Data availability

Data will be made available on request.

Acknowledgements

This work has received funding from the European Union's Horizon 2020 research and innovation program under the Marie Skłodowska-Curie grant agreement No 812909 CODOBIO, within the Marie Skłodowska-Curie International Training Networks framework.

Supplementary materials

Supplementary material associated with this article can be found, in the online version, at doi:10.1016/j.chroma.2024.464672.

References

[1] A.L. Grilo, A. Mantalaris, The increasingly human and profitable monoclonal antibody market, Trends Biotechnol. 37 (1) (2019) 9–16, https://doi.org/10.1016/j.tibtech.2018.05.014.
[2] G. Jagschies, E. Lindskog, K. Lacki, P.M. Galliher, Biopharmaceutical Processing: Development, Design, and Implementation of Manufacturing Processes, Elsevier, 2018, https://doi.org/10.1016/C2014-0-01092-1.
[3] A.A. Shukla, J. Thömmes, Recent advances in large-scale production of monoclonal antibodies and related proteins, Trends Biotechnol. 28 (5) (2010) 253–261, https://doi.org/10.1016/j.tibtech.2010.02.001.
[4] A.A. Shukla, B. Hubbard, T. Tressel, S. Guhan, D. Low, Downstream processing of monoclonal antibodies—Application of platform approaches, J. Chromatogr. B 848 (1) (2007) 28–39, https://doi.org/10.1016/j.jchromb.2006.09.026.
[5] S. Vunnum, G. Vedantham, B. Hubbard, Protein A-based affinity chromatography, in: U. Gottschalk (Ed.), Process Scale Purification Of Antibodies, John Wiley & Sons, Inc., USA and Canada, 2009, pp. 79–102, https://doi.org/10.1002/9780470444894.ch4.
[6] T. Ahamed, S. Chilamkurthi, B.K. Nfor, P.D. Verhaert, G.W. van Dedem, L.A. van der Wielen, M.H. Eppink, E.J. van de Sandt, M. Ottens, Selection of pH-related parameters in ion-exchange chromatography using pH-gradient operations, J. Chromatogr. A 1194 (1) (2008) 22–29, https://doi.org/10.1016/j.chroma.2007.11.111.
[7] G. Miesegaes, S. Lute, D. Strauss, E. Read, A. Venkiteshwaran, A. Kreuzman, R. Shah, P. Shamlou, D. Chen, Brorson, bioengineering, Monoclonal antibody capture and viral clearance by cation exchange chromatography, Biotechnol. Bioeng. 109 (8) (2012) 2048–2058, https://doi.org/10.1002/bit.24480.
[8] K.A. Kaleas, M. Tripodi, S. Revelli, V. Sharma, S.A. Pizarro, Evaluation of a multimodal resin for selective capture of CHO-derived monoclonal antibodies directly from harvested cell culture fluid, J. Chromatogr. B 969 (2014) 256–263, https://doi.org/10.1016/j.jchromb.2014.08.026.
[9] T. Hahn, N. Geng, K. Petrushevska-Seebach, M.E. Dolan, M. Scheindel, P. Graf, K. Takenaka, K. Izumida, L. Li, Z. Ma, Mechanistic modeling, simulation, and optimization of mixed-mode chromatography for an antibody polishing step, Biotechnol. Prog. (2022) e3316, https://doi.org/10.1002/btpr.3316.
[10] D.E. Steinmeyer, E.L. McCormick, The art of antibody process development, Drug Discov. Today 13 (13–14) (2008) 613–618, https://doi.org/10.1016/j.drudis.2008.04.005.
[11] D. Pfister, L. Nicoud, M. Morbidelli, Continuous Biopharmaceutical Processes: Chromatography, Bioconjugation, and Protein Stability, Cambridge University Press, 2018.
[12] T.C. Silva, M. Eppink, M. Ottens, Automation and miniaturization: enabling tools for fast, high-throughput process development in integrated continuous biomanufacturing, J. Chem. Technol. Biotechnol. (2021), https://doi.org/10.1002/jctb.6792.
[13] B.K. Nfor, M. Noverraz, S. Chilamkurthi, P.D. Verhaert, L.A. van der Wielen, M. Ottens, High-throughput isotherm determination and thermodynamic modeling of protein adsorption on mixed mode adsorbents, J. Chromatogr. A 1217 (44) (2010) 6829–6850, https://doi.org/10.1016/j.chroma.2010.07.069.

[14] M. Bensch, P. Schulze Wierling, E. von Lieres, J. Hubbuch, High throughput screening of chromatographic phases for rapid process development, Chem. Eng. Technol. 28 (11) (2005) 1274–1284, https://doi.org/10.1002/ceat.200500153.
[15] M. Wiendahl, P. Schulze Wierling, J. Nielsen, D. Fomsgaard Christensen, J. Krarup, A. Staby, J. Hubbuch, High throughput screening for the design and optimization of chromatographic processes – miniaturization, automation and parallelization of breakthrough and elution studies, Chem. Eng. Technol. 31 (6) (2008) 893–903, https://doi.org/10.1002/ceat.200800167.
[16] P.M. Schmidt, M. Abdo, R.E. Butcher, M.-Y. Yap, P.D. Scotney, M.L. Ramunno, G. Martin-Roussety, C. Owczarek, M.P. Hardy, C.-G. Chen, A robust robotic high-throughput antibody purification platform, J. Chromatogr. A 1455 (2016) 9–19. https://doi.org/10.1016/j.chroma.2016.05.076.
[17] J. Feliciano, A. Berrill, M. Ahnfelt, E. Brekkan, B. Evans, Z. Fung, R. Godavarti, K. Nilsson-Välimaa, J. Salm, U. Saplakoglu, Evaluating high-throughput scale-down chromatography platforms for increased process understanding, Eng. Life Sci. 16 (2) (2016) 169–178, https://doi.org/10.1002/elsc.201400241.
[18] A. Creasy, G. Barker, Y. Yao, G. Carta, Systematic interpolation method predicts protein chromatographic elution from batch isotherm data without a detailed mechanistic isotherm model, Biotechnol. J. 10 (9) (2015) 1400–1411, https://doi.org/10.1002/biot.201500089.
[19] T.M. Pabst, J. Thai, A.K. Hunter, Evaluation of recent Protein A stationary phase innovations for capture of biotherapeutics, J. Chromatogr. A 1554 (2018) 45–60, https://doi.org/10.1016/j.chroma.2018.03.060.
[20] T.C. Silva, M. Eppink, M. Ottens, Small, smaller, smallest: miniaturization of chromatographic process development, J. Chromatogr. A 1681 (2022) 463451, https://doi.org/10.1016/j.chroma.2022.463451.
[21] I.s.F. Pinto, R.R. Soares, S.A. Rosa, M.R. Aires-Barros, V. Chu, J.o.P. Conde, A. M. Azevedo, High-throughput nanoliter-scale analysis and optimization of multimodal chromatography for the capture of monoclonal antibodies, Anal. Chem. 88 (16) (2016) 7959–7967, https://doi.org/10.1021/acs.analchem.6b00781.
[22] A.T. Hanke, M. Ottens, Purifying biopharmaceuticals: knowledge-based chromatographic process development, Trends Biotechnol. 32 (4) (2014) 210–220, https://doi.org/10.1016/j.tibtech.2014.02.001.
[23] B.K. Nfor, P.D. Verhaert, L.A. van der Wielen, J. Hubbuch, M. Ottens, Rational and systematic protein purification process development: the next generation, Trends Biotechnol. 27 (12) (2009) 673–679, https://doi.org/10.1016/j.tibtech.2009.09.002.
[24] H. Schmidt-Traub, M. Schulte, A. Seidel-Morgenstern, H. Schmidt-Traub, Preparative Chromatography, Wiley Online Library, 2012, https://doi.org/10.1002/9783527816347.
[25] S.H. Altern, J.P. Welsh, J.Y. Lyall, A.J. Kocot, S. Burgess, V. Kumar, C. Williams, A. M. Lenhoff, S.M. Cramer, Isotherm model discrimination for multimodal chromatography using mechanistic models derived from high-throughput batch isotherm data, J. Chromatogr. A 1693 (2023) 463878, https://doi.org/10.1016/j.chroma.2023.463878.
[26] A. Seidel-Morgenstern, H. Schmidt-Traub, M. Michel, A. Epping, A. Jupke, Modeling and model parameters, Preparat. Chromatogr. (2012) 321–424, https://doi.org/10.1002/9783527649280.ch6.
[27] G. Carta, A. Jungbauer, Protein Chromatography: Process Development and Scale-Up, John Wiley & Sons, 2020, https://doi.org/10.1002/9783527630158.
[28] G. Guiochon, A. Felinger, D.G. Shirazi, Fundamentals of Preparative and Nonlinear Chromatography, Elsevier, 2006.
[29] B.K. Nfor, D.S. Zuluaga, P.J. Verheijen, P.D. Verhaert, L.A. van der Wielen, Marcel Ottens, Model-based rational strategy for chromatographic resin selection, Biotechnol. Prog. 27 (6) (2011) 1629–1643, https://doi.org/10.1002/btpr.691.
[30] S.M. Pirrung, D. Parruca da Cruz, A.T. Hanke, C. Berends, R.F. Van Beckhoven, M. H. Eppink, M. Ottens, Chromatographic parameter determination for complex biological feedstocks, Biotechnol. Prog. 34 (4) (2018) 1006–1018, https://doi.org/10.1002/btpr.2642.
[31] M. Moreno-González, D. Keulen, J. Gomis-Fons, G.L. Gomez, B. Nilsson, M. Ottens, Continuous adsorption in food industry: the recovery of sinapic acid from rapeseed meal extract, Sep. Purif. Technol. 254 (2021) 117403, https://doi.org/10.1016/j.seppur.2020.117403.
[32] F. Steinebach, M. Angarita, D.J. Karst, T. Müller-Späth, M. Morbidelli, Model based adaptive control of a continuous capture process for monoclonal antibodies production, J. Chromatogr. A 1444 (2016) 50–56, https://doi.org/10.1016/j.chroma.2016.03.014.
[33] M. Ostrihoňová, P. Cabadaj, M. Polakovič, Design of frontal chromatography separation of 1-phenylethanol and acetophenone using a hydrophobic resin, Sep. Purif. Technol. 314 (2023) 123578, https://doi.org/10.1016/j.seppur.2023.123578.
[34] C.A. Brooks, S.M. Cramer, Steric mass-action ion exchange: displacement profiles and induced salt gradients, AIChE J. 38 (12) (1992) 1969–1978, https://doi.org/10.1002/aic.690381212.
[35] Y.-C. Chen, S.-J. Yao, D.-Q. Lin, Parameter-by-parameter method for steric mass action model of ion exchange chromatography: theoretical considerations and experimental verification, J. Chromatogr. A 1680 (2022) 463418, https://doi.org/10.1016/j.chroma.2022.463418.
[36] M. Sokolov, M. von Stosch, H. Narayanan, F. Feidl, A. Butté, Hybrid modeling—a key enabler towards realizing digital twins in biopharma? Curr. Opin. Chem. Eng. 34 (2021) 100715 https://doi.org/10.1016/j.coche.2021.100715.
[37] R.M. Portela, C. Varsakelis, A. Richelle, N. Giannelos, J. Pence, S. Dessoy, M. von Stosch, When is an in silico representation a digital twin? A biopharmaceutical industry approach to the digital twin concept, Digital Twins: Tools Concept. Smart Biomanufactur. (2021) 35–55, https://doi.org/10.1007/10_2020_138.
[38] Y. Chen, O. Yang, C. Sampat, P. Bhalode, R. Ramachandran, M. Ierapetritou, Digital twins in pharmaceutical and biopharmaceutical manufacturing: a literature review, Processes 8 (9) (2020) 1088, https://doi.org/10.3390/pr8091088.
[39] A. Felinger, G. Guiochon, Comparison of the kinetic models of linear chromatography, Chromatographia 60 (1) (2004) S175–S180, https://doi.org/10.1365/s10337-004-0288-7.
[40] J. Van Deemter, F. Zuiderweg, A.v. Klinkenberg, Longitudinal diffusion and resistance to mass transfer as causes of nonideality in chromatography, Chem. Eng. Sci. 5 (6) (1956) 271–289, https://doi.org/10.1016/0009-2509(56)80003-1.
[41] P.V. Danckwerts, Continuous flow systems: distribution of residence times, Chem. Eng. Sci. 2 (1) (1953) 1–13, https://doi.org/10.1016/0009-2509(53)80001-1.
[42] M.N. São Pedro, M.H. Eppink, M. Ottens, Application of a fluorescent dye-based microfluidic sensor for real-time detection of mAb aggregates, Biotechnol. Prog. (2023) e3355, https://doi.org/10.1002/btpr.3355.
[43] T. Briskot, F. Stückler, F. Wittkopp, C. Williams, J. Yang, S. Konrad, K. Doninger, J. Griesbach, M. Bennecke, S. Hepbildikler, Prediction uncertainty assessment of chromatography models using Bayesian inference, J. Chromatogr. A 1587 (2019) 101–110, https://doi.org/10.1016/j.chroma.2018.11.076.
[44] V. Kumar, O. Khanal, M. Jin, Modeling the Impact of Holdup Volume from Chromatographic Workstations on Ion-Exchange Chromatography, Ind. Eng. Chem. Res. 61 (28) (2022) 10195–10204, https://doi.org/10.1021/acs.iecr.2c01266.
[45] W.K. Marek, D. Sauer, A. Dürauer, A. Jungbauer, W. Piątkowski, D. Antos, Prediction tool for loading, isocratic elution, gradient elution and scaling up of ion exchange chromatography of proteins, J. Chromatogr. A 1566 (2018) 89–101, https://doi.org/10.1016/j.chroma.2018.06.057.
[46] H.D. Young, Statistical Treatment of Experimental Data, McGraw-Hill Book Company, Inc., USA, 1962.
[47] D.A. Skoog, F.J. Holler, S.R. Crouch, Principles of instrumental analysis, Cengage Learn. (2017).
[48] TosohBiosciencesLLC, TOYOPEARL MX-Trp-650M - performance data, 2023. https://www.separations.us.tosohbioscience.com/Process_Media/id-7015/TOYOPEARL_MX-Trp-650M. (Accessed 03/07/2023 2023).
[49] A.R. Karow, S. Bahrenburg, P. Garidel, Buffer capacity of biologics—From buffer salts to buffering by antibodies, Biotechnol. Prog. 29 (2) (2013) 480–492, https://doi.org/10.1002/btpr.1682.
[50] B.C. de Neuville, A. Tarafder, M. Morbidelli, Distributed pore model for bio-molecule chromatography, J. Chromatogr. A 1298 (2013) 26–34, https://doi.org/10.1016/j.chroma.2013.04.074.
[51] F. Hagemann, P. Adametz, M. Wessling, V. Thom, Modeling hindered diffusion of antibodies in agarose beads considering pore size reduction due to adsorption, J. Chromatogr. A 1626 (2020) 461319, https://doi.org/10.1016/j.chroma.2020.461319.
[52] E. Müller, J. Vajda, Routes to improve binding capacities of affinity resins demonstrated for Protein A chromatography, J. Chromatogr. B 1021 (2016) 159–168, https://doi.org/10.1016/j.jchromb.2016.01.036.
[53] V. Natarajan, A.L. Zydney, Protein a chromatography at high titers, Biotechnol. Bioeng. 110 (9) (2013) 2445–2451, https://doi.org/10.1002/bit.24902.
[54] K. Swinnen, A. Krul, I. Van Goidsenhoven, N. Van Tichelt, A. Roosen, K. Van Houdt, Performance comparison of protein A affinity resins for the purification of monoclonal antibodies, J. Chromatogr. B 848 (1) (2007) 97–107, https://doi.org/10.1016/j.jchromb.2006.04.050.
[55] E.L. Cussler, Diffusion: Mass Transfer in Fluid Systems, 3rd ed., Cambridge University Press, USA, 2009.
[56] D.M. Ruthven, Principles of Adsorption and Adsorption Processes, John Wiley & Sons, USA and Canada, 1984.
[57] M. Yu, T.C. Silva, A. van Opstal, S. Romeijn, H.A. Every, W. Jiskoot, G.-J. Witkamp, M. Ottens, The investigation of protein diffusion via H-Cell microfluidics, Biophys. J. 116 (4) (2019) 595–609, https://doi.org/10.1016/j.bpj.2019.01.014.
[58] S. Golshan-Shirazi, G. Guiochon, Comparison of the various kinetic models of non-linear chromatography, J. Chromatogr. A 603 (1–2) (1992) 1–11, https://doi.org/10.1016/0021-9673(92)85340.
[59] N.K. Hiester, T. Vermeulen, Saturation performance of ion exchange and adsorption columns, Chem. Eng. Prog. 48 (10) (1952) 505–516.
[60] M.D. LeVan, G. Carta, Adsorption and ion exchange, in: D.W. Green (Ed.), Perry's Chemical Engineers' Handbook, McGraw-Hill, New York, 2008, 16-1-16-54.
[61] C.-S. Chen, F. Konoike, N. Yoshimoto, S. Yamamoto, A regressive approach to the design of continuous capture process with multi-column chromatography for monoclonal antibodies, J. Chromatogr. A 1658 (2021) 462604, https://doi.org/10.1016/j.chroma.2021.462604.
[62] R. Hahn, P. Bauerhansl, K. Shimahara, C. Wizniewski, A. Tscheliessnig, A. Jungbauer, Comparison of protein A affinity sorbents: II. Mass transfer properties, J. Chromatogr. A 1093 (1–2) (2005) 98–110, https://doi.org/10.1016/j.chroma.2005.07.050.
[63] A.S. Rathore, S. Nikita, G. Thakur, S. Mishra, Artificial intelligence and machine learning applications in biopharmaceutical manufacturing, Trends Biotechnol. (2022), https://doi.org/10.1016/j.tibtech.2022.08.007.
[64] A.S. Rathore, S. Nikita, G. Thakur, N. Deore, Challenges in process control for continuous processing for production of monoclonal antibody products, Curr. Opin. Chem. Eng. 31 (2021) 100671. https://doi.org/10.1016/j.coche.2021.100671.